

## Simple model for bursting dynamics of neurons

Anandamohan Ghosh,<sup>\*</sup> Dipanjan Roy,<sup>†</sup> and Viktor K. Jirsa<sup>‡</sup>  
*Theoretical Neuroscience Group, Institut des Sciences du Mouvement, UMR 6233, CNRS  
 and Université de la Méditerranée, 163 Avenue de Luminy, 13288 Marseille, France*

(Received 22 May 2009; revised manuscript received 26 September 2009; published 29 October 2009)

Neuronal cells in isolation or as an assembly exhibit bursting behavior on two different time scales. We introduce a simple one-dimensional model which requires only one phase variable to describe the phenomenon of parabolic bursting. The analysis in the continuum limit reveals that for any unimodal distribution of frequencies, the qualitative properties of the full and the reduced model are identical. Further, we derive analytically an exact low-dimensional description of a globally coupled network of bursting oscillators for our model. Study of the stability for this low-dimensional model reveals different dynamical signatures in the parameter space. We demonstrate that the structure of the parameter space remains independent of the number of spikes per burst.

DOI: [10.1103/PhysRevE.80.041930](https://doi.org/10.1103/PhysRevE.80.041930)

PACS number(s): 87.19.1l, 87.19.lj, 87.19.lm

Bursting is a dynamic phenomenon that alternates between slowly changing quiescent states and periods of activity. Neuronal cells, whether in isolation or part of an assembly, exhibit such behavior and the study of generating mechanisms for bursting is an area of active research [1–6]. Neural bursting can occur due to external forcing or due to interplay of fast and slow time scales of the system [7]. Specifically in *parabolic bursting*, at the start and end of the active phase the spike frequency is smaller compared to the middle of the active phase. This type of bursting has been observed in the R-15 neuron in abdominal ganglion of *Aplysia* and has been qualitatively modeled and studied [8]. Parabolic bursting is modeled using either three- or two-dimensional nonlinear dynamic systems, of which the latter has been shown to be reducible to a canonical form [9]. In this paper we introduce a simple one-dimensional phase model, which captures all the characteristics of parabolic bursting. Integrated in small networks analytical techniques become applicable due to the model's simplicity, whereas large bursting network models will benefit from the fact that it is simple to integrate and computationally inexpensive. As an example, we will study a population of bursters with phase coupling and derive an exact low-dimensional description for the complex order parameter of the population displaying bifurcation phase diagram with the different types of synchronization. In previous studies, similar couplings have been used in populations of coupled limit cycle oscillators (Kuramoto oscillators) in the context of pacemaker cells in the heart, circadian behavior of neural cells in the brain, and others [10,11]. This paper is organized as follows: first we formally introduce our model, then we present our results of network dynamics of globally coupled network of oscillators; subsequently we derive a low-dimensional reduced system in the continuum limit and study the bifurcations of the reduced system.

The class of models that has been shown to exhibit parabolic bursting can be generically represented in the following form:

$$\dot{x} = f(x) + \epsilon^2 g(x, y, \epsilon), \quad (1)$$

$$\dot{y} = \epsilon h(x, y, \epsilon), \quad (2)$$

where  $x \in \mathbb{R}^n$ ,  $y \in \mathbb{R}^m$  and for smooth functions  $f, g, h$  and  $\epsilon \ll 1$  it has been shown that burstlike solutions exist under the assumptions: (a)  $\dot{x} = f(x)$  has an attracting invariant circle and (b)  $\dot{y} = h(0, y, 0)$  has a stable limit cycle solution [9]. It has also been shown that the canonical form of the bursting equations written in terms of phase variable  $\theta \in \mathbb{S}^1$  assumes the form

$$\dot{\theta} = (1 - \cos \theta) + (1 + \cos \theta) \sin \psi, \quad (3)$$

$$\dot{\psi} = \omega, \quad (4)$$

where  $\sin(\psi)$  is the slowly varying periodic driving [9]. Essentially the canonical form is of the following form:

$$\dot{\theta} = 1 - \cos \theta + A(x, y), \quad (5)$$

$$\dot{x} = \epsilon_x [x_\alpha(\theta) - x]; \quad \dot{y} = \epsilon_y [y_\alpha(\theta) - y], \quad (6)$$

where  $A(x, y)$  is an activation function dependent on the slow variables  $(x, y)$  of the system [7]. The function  $A(x, y)$  is a smoothly varying periodic function changing signs such that the system alternately undergoes saddle node on an invariant circle bifurcation. The slow variables  $A(x, y)$  determines the bifurcation pattern as shown in Fig. 1.

In the above class of models the fast subsystem is driven by a slow subsystem involving a separate dynamical subsystem for the slow variables. In this paper we propose a model that shows parabolic bursting involving only the phase variable  $\theta$ ,

$$\dot{\theta} = a - \cos(\theta) - \cos(\theta/n), \quad (7)$$

where  $\cos(\theta/n)$  is the slow term,  $a$  being the bifurcation parameter and  $n$  determines the number of spikes per burst.

<sup>\*</sup>anandamohan.ghosh@univmed.fr

<sup>†</sup>dipanjan.roy@etumel.univmed.fr

<sup>‡</sup>viktor.jirsa@univmed.fr

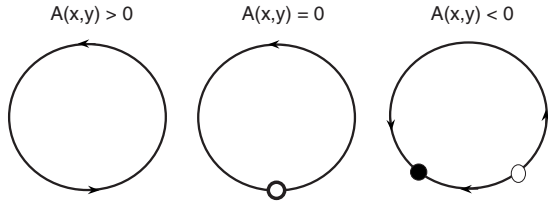


FIG. 1. Saddle-node bifurcation on an invariant circle. Black dot, open circle, and thick open circle indicates stable, unstable, and semistable fixed points, respectively.

Without the slow term the system shows saddle node bifurcation on an invariant circle. Incorporating the slow term the dynamics rides on the slowly varying sinusoidal function and burst/spikes and interburst intervals are governed by the fast term and slow term, respectively. For  $a > 2$  all the fixed points have imaginary values giving rise to oscillatory behavior and the time period of oscillations can be obtained as follows: Let  $\phi = \theta - \theta^*$  be the deviation from the fixed point  $\theta^*$  and Eq. (7) gives

$$\dot{\phi} = a - \cos(\phi) - \cos\left(\frac{\phi}{n}\right) = a - 2 + \frac{n^2 + 1}{2n^2} \phi^2 + h.o. \quad (8)$$

Let  $r = a - 2$  and  $x = \sqrt{(n^2 + 1)/2n^2} \phi$  then  $\tau \dot{x} = r + x^2$ , where  $\tau = \sqrt{2n^2/(n^2 + 1)}$ . The time period  $T$  is

$$T = \tau \int_{-\infty}^{+\infty} \frac{dx}{r + x^2} = \tau \frac{\pi}{\sqrt{a - 2}}. \quad (9)$$

It is easy to see that as  $a \rightarrow 2$ , time period  $T \rightarrow \infty$ . Thus by tuning the control parameter it is possible to obtain parabolic bursts separated by our desired interburst gap. The time evolution of a single oscillator is shown in Fig. 2(a), where a voltage-like quantity  $V = -\cos \theta$ , plotted as a function of time, shows the regular parabolic bursting. We have introduced inter burst variability by adding noise in Eq. (7). In Fig. 2(b) we show the time evolution of the stochastic version of Eq. (7) which is integrated with noise using Euler-Maruyama method [13]. The noise allows interburst interval to vary and is determined by the noise strength,  $\mu$ .

Now we study the effect of coupling on a network of bursting oscillators. The coupled system with stochastic time evolution can be written as

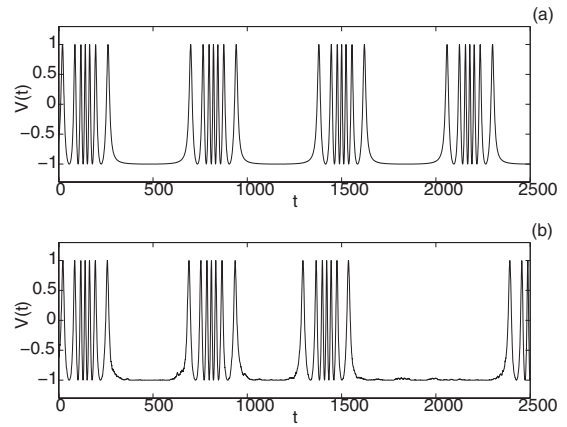


FIG. 2.  $V(t) = -\cos[\theta(t)]$  is plotted as a function of time in arbitrary units,  $a = 2.01$ ,  $n = 7$ ; (a) without noise, (b) with noise, noise strength  $\mu = 0.02$ .

$$d\theta_i = \left[ a_i - F(\cos(\theta_i) + \cos(\theta_i/n)) + \frac{\epsilon}{M} \sum_{j=1}^M \sin(\theta_i - \theta_j) \right] dt + \mu dW_i, \quad (10)$$

where  $\epsilon$  is the coupling strength,  $F$  is the forcing strength,  $M$  is the number of oscillators, and  $dW_i$  denotes a Weiner process. The synchronized behavior can be studied by computing a complex order parameter defined as  $R(t) = \frac{1}{M} \sum_j \exp[i\theta_j(t)]$ , where for a synchronized state  $|R| = 1$  and for a completely unsynchronized state  $|R| \approx 0$  for large  $n, M$ . First we consider two coupled oscillators and show the time evolution of  $V(t)$  for  $\epsilon = 0.2$  and  $\epsilon = 2.0$ ,  $a_1 = a_2 = 2.01$  and  $F = 1.0$  (Fig. 3). For random choice of initial phases and for  $\epsilon = 0.0$ ,  $V(t)$  evolves independently, implying  $|R(t)| \ll 1$ . For  $\epsilon = 0.2$  after a few initial transients the bursts synchronize but the spikes do not as reflected in the behavior of the order parameter  $R(t)$ . For high coupling strength  $\epsilon = 2.0$  there is complete synchronization and the order parameter stays close to 1 for all times. The variation in coupling strength results in a transition to the synchronized state from the completely unsynchronized state. The phase transition is demonstrated for an all-to-all coupled network for varying  $n$  (Fig. 4).

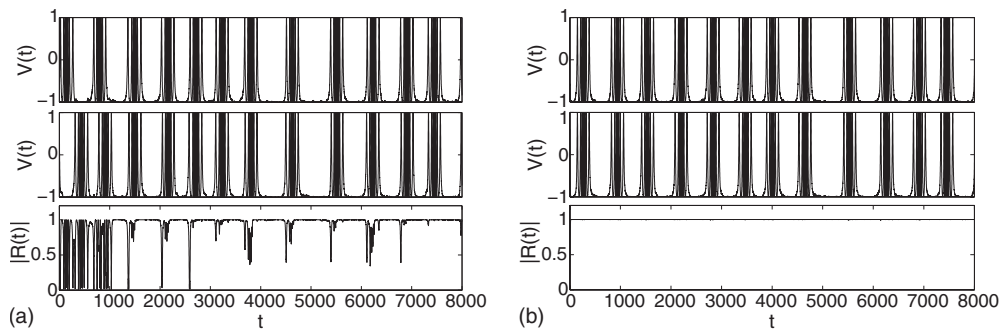


FIG. 3. The temporal dynamics of two coupled bursters is shown in first and second row. The third row shows the order parameter for coupling strength; (a) left:  $\epsilon = 0.2$ , burst synchronization; (b) right:  $\epsilon = 2.0$ , spike synchronization. Other parameters are chosen as in Fig. 2.

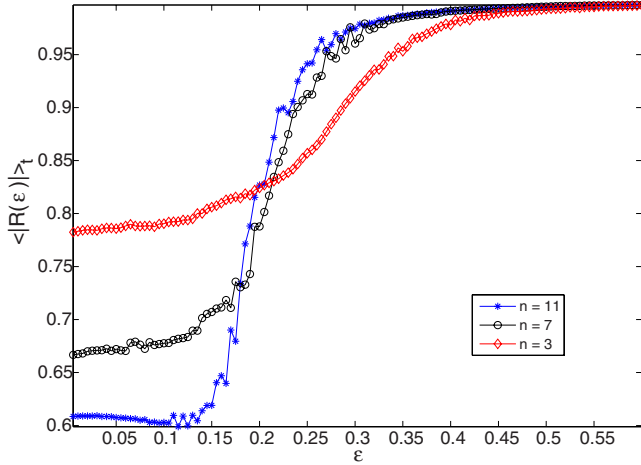


FIG. 4. (Color online) Time averaged order parameter  $\langle |R(\epsilon)| \rangle$ , is plotted as a function of coupling strength,  $\epsilon$ , for varying  $n$ . Number of bursters,  $M=100$ .

The analysis of phase oscillators is often done in the continuum limit ( $M \rightarrow \infty$ ), where the state of the coupled system can be described by a density function  $f(\theta, a, t)$ , where  $f$  is defined such that the fraction of oscillators with phases lying between  $\theta$  and  $d\theta$  and frequencies between  $a$  and  $da$  is given by  $f(\theta, a, t)d\theta da$  [10,14]. The natural frequencies are drawn from a distribution  $g(a)$  such that

$$\int_{-\infty}^{\infty} \int_0^{2\pi} f(\theta, a, t) d\theta da = 1, \quad \int_0^{2\pi} f(\theta, a, t) d\theta = g(a) \quad (11)$$

For the conservation of oscillators of frequency  $a$  the continuity equation is written as

$$\frac{\partial f}{\partial t} + \frac{\partial(fv)}{\partial \theta} = 0. \quad (12)$$

The velocity  $v(\theta, a, t) = d\theta/dt$  is now written as

$$v(\theta, a, t) = a - F \sin(\theta) - F \sin(\theta/n) + \epsilon \int_{-\infty}^{\infty} \int_0^{2\pi} \sin(\hat{\theta} - \theta) f(\hat{\theta}, \hat{a}, t) d\hat{\theta} d\hat{a}, \quad (13)$$

where without loss of any generality but for analytic simplicity we use sin functions instead of cos functions in Eq. (7).

In the continuum limit the complex order parameter  $z$  can be defined as

$$z(t) = \int_{-\infty}^{\infty} \int_0^{2\pi} e^{i\theta} f(\theta, a, t) d\theta da. \quad (14)$$

Using the above it is easy to see that the expression for the velocity becomes

$$v(\theta, a, t) = a - F \left( \frac{e^{i\theta/n}}{2i} - \frac{e^{-i\theta/n}}{2i} \right) + \frac{1}{2i} [(\epsilon z + F)e^{-i\theta} - (\epsilon z + F)^* e^{i\theta}], \quad (15)$$

where  $\star$  indicates the complex conjugate. The distribution function can be expressed as a Fourier series

$$f(\theta, a, t) = \frac{g(a)}{2\pi} \left[ 1 + \sum_{k=1}^{\infty} f_k(a, t) e^{ik\theta} + c.c. \right]. \quad (16)$$

The above infinite-dimensional system is difficult to analyze. However, the ansatz of Ott and Antonsen [12] has been shown to be successful in obtaining the low-dimensional description of the globally coupled phase oscillators. The ansatz imposes a restriction on the Fourier coefficients  $f_k(a, t) = [\psi(a, t)]^k$  for  $k \geq 1$  and has been shown to be a reasonable guess under different scenarios [12]. This restricted class of functions readily reduces our continuity equation to an  $\theta$ -independent form

$$\frac{dz}{dt} = \frac{1}{2}(\epsilon z + F)^* - ia\psi - \frac{1}{2}(\epsilon z + F)\psi^2 - F \left( \frac{\psi^{1+1/n}}{2} - \frac{\psi^{1-1/n}}{2} \right), \quad (17)$$

with  $z$  satisfying  $z(t) = \int_{-\infty}^{\infty} \psi^*(a, t) g(a) da$ . If we assume a Lorentzian distribution  $g(a) = 1/\pi[(a-a_0)^2 + 1]$ .  $z(t)$  can be evaluated by contour integration with poles at  $a = a_0 - i$  and we obtain the exact evolution equation of order parameter  $z$ ,

$$\frac{dz}{dt} = ia_0 z - z + \frac{\epsilon z + F}{2} - \left( \frac{\epsilon z^* + F}{2} \right) z^2 - F \left( \frac{z^{1+1/n}}{2} - \frac{z^{1-1/n}}{2} \right). \quad (18)$$

The above equation can be expressed in polar coordinates if we substitute  $z = \rho \exp(i\phi)$ , giving evolution equations for  $\rho$  and  $\phi$ ,

$$\frac{d\rho}{dt} = \frac{\epsilon}{2}\rho(1 - \rho^2) - \rho + \frac{F}{2}(1 - \rho^2)\cos \phi + \frac{F\rho}{2}(\rho^{-1/n} - \rho^{1/n})\cos\left(\frac{\phi}{n}\right), \quad (19)$$

$$\frac{d\phi}{dt} = a_0 - \frac{F}{2}\left(\rho + \frac{1}{\rho}\right)\sin \phi - \frac{F}{2}\left(\rho^{1/n} + \frac{1}{\rho^{1/n}}\right)\sin\left(\frac{\phi}{n}\right). \quad (20)$$

For the Lorentzian distribution the above equation is exact; however, for arbitrary unimodal distributions of frequencies we have not seen any qualitative differences in the behavior of the reduced model and the full model.

For the choice of  $n=1$  and  $F=2$  the Eqs. (25) and (26) are identical to the reduced equations studied by Childs *et al.* [15]. On the other hand, retaining  $F$  but setting  $n=1$  we obtain a similar set of equations except a factor of half which results in no qualitative difference in the bifurcation diagram as in Childs *et al.* [15] other than shifting the values in the  $(a_0, F)$  parameter plane. The above set of equations is diffi-

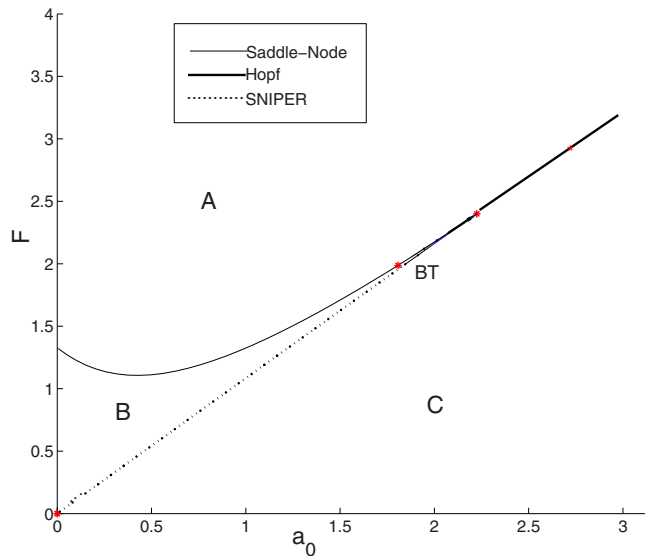


FIG. 5. (Color online) Stability diagram for the reduced model in the parameter plane  $(a_0, F)$  for coupling constant  $\epsilon=4.0$  and number of spikes  $n=2$ . BT denotes the Takens-Bogdanov point.

cult to study analytically for  $n > 1$ . We present here the numerical studies carried out for the above set of equations and are mainly interested in characterizing the different dynamical regimes for the reduced system. In order to obtain the stability diagram in the  $(a_0, F)$  parameter plane (Fig. 5) we employ the following scheme: determine the saddle node bifurcation curve by imposing the conditions  $d\rho/dt=0$ ,  $d\phi/dt=0$ ,  $\text{Det } J=0$ , where  $J$  is the Jacobian matrix. Solving these simultaneously and sweeping  $\rho$  and  $\phi$  over their full ranges  $0 \leq \rho \leq 1$ ,  $-\pi \leq \phi \leq \pi$  we consider pairs of values of  $(a_0, F)$  that are positive. Similarly we determine the Hopf bifurcation curve by imposing the conditions  $d\rho/dt=0$ ,  $d\phi/dt=0$ ,  $\text{Tr } J=0$ . The bifurcation curves can also be obtained by using the MATLAB numerical continuation package MATCONT [16]. The selection of  $\epsilon$  is guided by the choices made in the previous studies by [12,15]. For coupling constant  $\epsilon=4.0$  and  $n=1, \dots, 9$  the bifurcation diagram remains identical as shown in Fig. 5 for the case when  $n=2$ . The study of the bifurcation properties for  $n=2$  is sufficient as we

find the local dynamics is independent of the number of spikes. The stability diagram is divided mainly in three regions, A, B, and C, by the bifurcation curves labeled Saddle node, Hopf, and SNIPER (saddle node infinite period bifurcation). In the region A the order parameter approaches a stable fixed point, implying that the dynamics is phase locked to the driving term. The region B also shows forced entrainment. Forced entrainment is lost in region C, which has a globally attracting limit cycle with stable period. The phase of the order parameter increases monotonically relative to the forcing parameter  $F$  and the system entrains itself mutually [15,17]. Moreover, we observe that the two branches of the saddle curve and the Hopf curve intersect tangentially, which necessitates the presence of a Takens-Bogdanov point. Takens-Bogdanov point also implies that there will be a emergent homoclinic orbit as a result of a global bifurcation [18]. Thus there will be a region where there coexists a saddle and a limit cycle implying bistability. However, in our numerically evaluated bifurcation diagram this occurs in a very small region and the homoclinic orbit is difficult to identify and remains a problem for future studies.

In this paper we studied the mechanism of parabolic bursting phenomena using a simple phase model. This model has inherent simplicity in comparison to earlier models as it requires only one phase variable to capture all the qualitative properties of bursting phenomena. On the one hand, for a neuronal network composed of identical units of such phase oscillators it allows mathematical tractability and, on the other hand, reduces significant amount of computational complexity. Furthermore, as the number of spikes per burst increases the scope of analytical study becomes generally restricted. Here we demonstrated that for a fixed coupling strength the parameter space structure remains independent of the number of spikes per burst. This allows to study the network model for single spike bursts and infer the local dynamics of the coupled more general multispikes system.

#### ACKNOWLEDGMENTS

This research has been supported by the ATIP Plus Program (CNRS), Program Neuroinformatique (CNRS), and the JS McDonnell Foundation.

- 
- [1] J. Rinzel and Y. S. Lee, *Nonlinear Oscillations in Biology and Chemistry* (MIT Press, Cambridge, 1986).
- [2] J. Rinzel, in *Mathematical Topics in Population Biology, Morphogenesis, and Neurosciences*, edited by E. Teramoto and M. Yamaguti, Lecture Notes in Biomathematics Vol. 71 (Springer-Verlag, Berlin, 1987).
- [3] J. Rinzel and G. B. Ermentrout, in *Analysis of Neuronal Excitability and Oscillations*, edited by C. Koch and I. Segev, Methods in Neuronal Modeling (MIT Press, Cambridge, 1989).
- [4] J. Hindmarsh and P. Cornelius, in *Bursting: The Genesis of Rhythm in the Nervous System*, edited by S. Coombes and P. C. Bressloff (World Scientific, Singapore, 2005).
- [5] E. M. Izhikevich, *Dynamical Systems in Neuroscience: The Geometry of Excitability and Bursting* (MIT Press, Cambridge, 2006).
- [6] E. M. Izhikevich, *Int. J. Bifurcation Chaos Appl. Sci. Eng.* **10**, 1171 (2000).
- [7] S. M. Baer, J. Rinzel, and H. Carrillo, *J. Math. Biol.* **33**, 309 (1995).
- [8] R. E. Plant, *J. Math. Biol.* **11**, 15 (1981).
- [9] G. B. Ermentrout and N. Kopell, *SIAM J. Appl. Math.* **46**, 233 (1986).
- [10] S. H. Strogatz, *Physica D* **143**, 1 (2000).
- [11] D. Cumin and C. P. Unsworth, *Physica D* **226**, 181 (2007).
- [12] E. Ott and T. A. Antonsen, *Chaos* **18**, 037113 (2008).
- [13] D. J. Higham, *SIAM Rev.* **43**, 525 (2001).

- [14] T. M. Antonsen, R. T. Faghih, M. Girvan, E. Ott, and J. Platig, *Chaos* **18**, 037112 (2008).
- [15] M. L. Childs and S. H. Strogatz, *Chaos* **18**, 043128 (2008).
- [16] MATCONT is freely available at <http://www.matcont.UGent.be>
- [17] H. Daido, *Phys. Rev. Lett.* **73**, 760 (1994).
- [18] S. Wiggins, *Introduction to Applied Nonlinear Dynamics and Chaos Texts in Applied Mathematics* (Springer-Verlag, Berlin, 2003), Vol. 2.